Published for SISSA by Springer

Received: August 12, 2022
Accepted: October 17, 2022
Published: October 28, 2022

Top-Yukawa-induced corrections to Higgs pair production

Margarete Mühlleitner,[a] Johannes Schlenk[b] and Michael Spira[b]

[a] *Institute for Theoretical Physics, Karlsruhe Institute of Technology, Wolfgang-Gaede-Str. 1, D-76131 Karlsruhe, Germany*
[b] *Theory Group LTP, Paul Scherrer Institut, Forschungsstrasse 111, CH-5232 Villigen PSI, Switzerland*

E-mail: milada.muehlleitner@kit.edu, johannes.schlenk@psi.ch, michael.spira@psi.ch

Abstract: Higgs-boson pair production at hadron colliders is dominantly mediated by the loop-induced gluon-fusion process $gg \to HH$ that is generated by heavy top loops within the Standard Model with a minor per-cent level contamination of bottom-loop contributions. The QCD corrections turn out to be large for this process. In this note, we derive the top-Yukawa-induced part of the electroweak corrections to this process and discuss their relation to an effective trilinear Higgs coupling with integrated out top-quark contributions.

Keywords: Higgs Properties, Higher Order Electroweak Calculations, Electroweak Precision Physics

ArXiv ePrint: 2207.02524

https://doi.org/10.1007/JHEP10(2022)185

Contents

1 Introduction

The discovery of a bosonic particle with a mass of (125.09 ± 0.24) GeV [1, 2] turned out to be in agreement with the Standard-Model (SM) Higgs boson within the present uncertainties of all production and decay modes. Its coupling strengths to SM gauge bosons, i.e. ZZ, W^+W^-, and fermion pairs as τ, μ leptons and bottom quarks as well as the loop-induced couplings to gluon and photon pairs, have been measured with accuracies of $10-50\%$. All measurements are in agreement with the SM predictions within their uncertainties [3–5]. In addition, there are very strong indications that the newly discovered boson carries zero spin and positive CP-parity, i.e. possible deviations from these hypotheses are strongly constrained by the accuracy of present experimental data. Thus, there is increasing evidence that this particle is indeed the long-sought SM Higgs boson. Its discovery is of vital importance for the consistency of the SM and the success of the predictions for the precision electroweak observables which are in striking agreement with measurements at LEP and SLC [6]. The discovery of a SM-like Higgs boson at the LHC completed the SM of electroweak and strong interactions. The existence of the Higgs boson is inherently related to the mechanism of spontaneous symmetry breaking while preserving the full gauge symmetry and the renormalizability of the SM [7, 8], since the Higgs boson permits the SM particles to be weakly interacting up to high-energy scales [9–12]. However, with the knowledge of the Higgs-boson mass all its properties within the SM are uniquely fixed, i.e. the SM does not allow the Higgs couplings to the SM particles to deviate from their unique predictions.

The minimal model as realized in the SM requires the introduction of one isospin doublet of Higgs fields that leads after spontaneous symmetry breaking to the existence of one scalar Higgs boson. A crucial experimental goal is the measurement of the Higgs potential, since the formation of a non-trivial ground state with a finite vacuum expectation value of the Higgs field causes electroweak symmetry breaking so that the experimental verification of the Higgs potential itself is of highest interest. The parameters describing the Higgs potential are the Higgs mass and self-interactions of the Higgs field. The production of Higgs-boson pairs is the first class of processes that offers the direct access to the trilinear self-coupling of the Higgs boson as a first step towards the reconstruction of the full Higgs potential. At the Large Hadron Collider (LHC), the dominant Higgs-boson pair production mechanism is provided by the gluon-fusion process $gg \to HH$, while the other production modes as vector-boson fusion (VBF) $qq \to qqHH$, double Higgs-strahlung $q\bar{q} \to W/Z+HH$ and double Higgs bremsstrahlung off top quarks $q\bar{q}, gg \to t\bar{t}HH$ are suppressed by at least one order of magnitude [13, 14]. The individual production cross sections roughly follow the pattern of single-Higgs boson production but are in general smaller by about three orders of magnitude. Since the trilinear Higgs coupling contributes only to a subset of diagrams of each production process the sensitivity to the trilinear Higgs coupling is reduced due to the dominance of the continuum diagrams. The slope of the gluon-fusion cross section as a function of the trilinear Higgs coupling λ follows the rough behaviour $\Delta\sigma/\sigma \sim -\Delta\lambda/\lambda$ around the SM prediction [13–16]. This implies that the uncertainties of the production cross section are immediately translated to the uncertainties of the extracted trilinear self-coupling so that the reduction of the theoretical uncertainties of the Higgs pair production cross section is crucial for an accurate extraction of the trilinear self-interaction from the experimental measurements. This feature translates to a similar situation for the distributions as well. The trilinear coupling develops a significant contribution for Higgs-pair production closer to the production threshold, while it dies out for large invariant Higgs-pair masses. In the last range, however, statistics will be small in experiment so that the bulk of reconstructed events will emerge from the region closer to the threshold.

The gluon-fusion mechanism $gg \to HH$ is mediated by top- and to a much lesser extent bottom-quark loops, see figure 1. The full next-to-leading-order (NLO) QCD corrections have been calculated by a time-consuming numerical integration of the corresponding two-loop integrals, since there are no systematic analytical methods to calculate the corresponding two-loop integrals [17–21]. Similar to the single-Higgs case they enhance the cross section by about 70%. Because the invariant mass of the final-state Higgs-boson pair is significantly larger than in the single-Higgs case, the heavy top-quark limit (HTL) works less reliably for Higgs-boson pairs. The full NLO QCD corrections result in a decrease of the total cross section by about 15%, due to finite NLO top mass effects beyond the heavy-top limit, at the LHC for a c.m. energy of 14 TeV. This shows that the heavy-top limit for the relative QCD corrections [15] works still quite well for the total cross section also in the Higgs-pair case. For the exclusive cross section at large invariant Higgs-pair masses, however, the finite mass effects at NLO can reach a level of −30%. The next-to-NLO (NNLO) QCD corrections to the total cross section have been obtained in the heavy top-quark limit. They imply an additional moderate rise of the total cross section by about 20% [22–25]. Recently, the next-to-NNLO (N^3LO) QCD corrections to the total cross section became available and turned out to be small, affecting the total cross section at the few per-cent level only [26, 27]. NNLO top mass effects have been estimated to about 5% by means of a heavy top-quark expansion of the 2-loop virtual corrections [28].

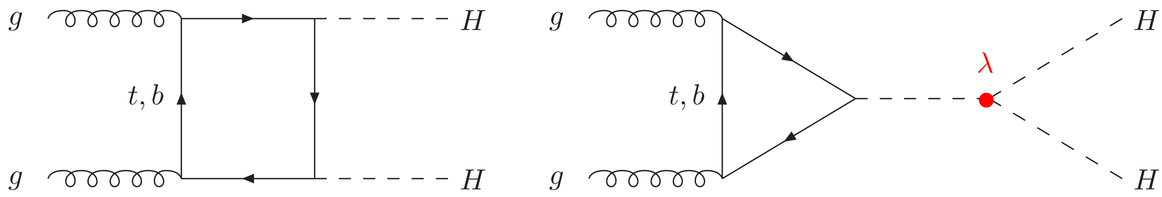

Figure 1. Diagrams contributing to Higgs-boson pair production via gluon fusion. The contribution of the trilinear Higgs coupling is marked in red.

Beyond NNLO, the next-to-next-to-leading-logarithmic (NNLL) soft and collinear gluon resummation contributes 5–10% to the total cross section [29, 30]. The factorization and renormalization scale dependence has been reduced to about 5%. In order to obtain an estimate of the residual theoretical uncertainties, however, the uncertainties due to the scheme and scale choice of the virtual top mass have to be taken into account as well. These latter effects increase the theoretical uncertainties to a level of 20–25% [19–21]. The electroweak corrections to this process are unknown. They are expected in the 10%-range for the total cross section, but larger in the tails of the distributions.

In this work we investigate the electroweak corrections induced by the top-Yukawa coupling as a uniquely defined contribution to the full electroweak corrections. In section 2, we will define our notation and the corresponding leading-order (LO) result for $gg \to HH$. In section 3, we describe the effective Higgs (pair) couplings to gluons in the HTL and the effective trilinear Higgs coupling within the effective-potential approach, where the top contributions are integrated out. Section 4 describes the NLO calculation and section 5 our results with a discussion of our findings. In section 6, we conclude.

2 Higgs-boson pair production at leading order

The LO Higgs pair production via gluon fusion is mediated by heavy top-loop contributions and a marginal contribution of bottom loops, see figure 1. In this work we neglect the bottom-loop contributions and take into account the top loops only. The Higgs-boson pair production cross section at LO is given by

$$\sigma_{\rm LO} = \int_{\tau_0}^1 d\tau \, \frac{d\mathcal{L}^{gg}}{d\tau} \, \hat\sigma_{\rm LO}(Q^2 = \tau s)\,, \tag{2.1}$$

where $\mathcal{L}^{gg}$ denotes the gluonic parton luminosity given in terms of the gluon densities $g(x, \mu_F)$,

$$\frac{d\mathcal{L}^{gg}}{d\tau} = \int_\tau^1 \frac{dx}{x} g(x,\mu_F) g\left(\frac{\tau}{x}, \mu_F\right) \tag{2.2}$$

at the factorization scale μ_F, and the integration boundary is given by $\tau_0 = 4M_H^2/s$, where s denotes the hadronic center-of-mass (c.m.) energy squared and M_H the Higgs mass. The scale $Q^2 = M_{HH}^2$ is defined in terms of the invariant mass M_{HH} of the Higgs pair at LO.

JHEP10(2022)185

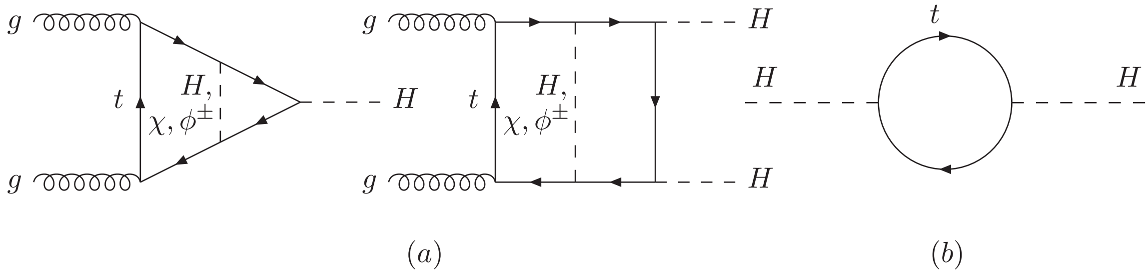

Figure 2. Typical diagrams contributing to the top-Yukawa-induced electroweak corrections to the effective Lagrangian: (a) vertex corrections, (b) wave-function corrections. The fields $\chi, \phi^\pm$ denote the pseudoscalar and charged would-be Goldstones.

The LO partonic cross section can be cast into the form

$$\hat{\sigma}_{LO} = \frac{G_F^2 \alpha_s^2(\mu_R)}{512(2\pi)^3} \int_{\hat{t}_-}^{\hat{t}_+} d\hat{t} \Big[|C_\triangle F_\triangle + F_\Box|^2 + |G_\Box|^2 \Big] , \tag{2.3}$$

where the integration boundaries are given by

$$\hat{t}_\pm = -\frac{1}{2} \left[Q^2 - 2M_H^2 \mp Q^2 \sqrt{1 - 4\frac{M_H^2}{Q^2}} \right] , \tag{2.4}$$

and the symmetry factor 1/2 for the identical Higgs bosons in the final state is included. The coefficient $C_\triangle = \lambda_{HHH} v/(Q^2 - M_H^2)$ involves the trilinear Higgs coupling that is related to the Higgs mass and the vacuum expectation value (vev) v at LO,

$$\lambda_{HHH} = 3\frac{M_H^2}{v} , \tag{2.5}$$

where the vev is related to the Fermi constant $G_F = 1/(\sqrt{2} v^2)$. The factor $\alpha_s(\mu_R)$ denotes the strong coupling at the renormalization scale μ_R. The form factors $F_\triangle$ of the LO triangle diagrams and $F_\Box, G_\Box$ of the LO box diagrams can be found in refs. [31, 32]. In the HTL they approach simple expressions, $F_\triangle \to 2/3$, $F_\Box \to -2/3$ and $G_\Box \to 0$.

3 Effective Lagrangians

In this section we address the effective gluonic single- and double-Higgs couplings as well as the effective Higgs self-couplings after integrating out the heavy-top contributions, i.e. the effective couplings valid in the HTL at the leading order of an inverse large top-mass expansion.

3.1 Gluonic Higgs couplings

In the HTL, the top-Yukawa-induced electroweak corrections to the effective Hgg and $HHgg$ couplings can be obtained as

$$\mathcal{L}_{\rm eff} = C_1 \frac{\alpha_s}{12\pi} G^{a\mu\nu} G^a_{\mu\nu} \log\left(1 + C_2 \frac{H}{v}\right) , \tag{3.1}$$

where $G^a_{\mu\nu}$ denotes the gluonic field-strength tensor and H the SM Higgs field. The radiatively corrected coefficients are given by

$$
\begin{aligned}
C_1 &= 1 - 3x_t + \mathcal{O}(x_t^2) \\
C_2 &= 1 + \frac{7}{2}x_t + \mathcal{O}(x_t^2)\,,
\end{aligned} \tag{3.2}
$$

with $x_t = G_F m_t^2/(8\sqrt{2}\pi^2)$, where C_1 describes the genuine corrections to the Hgg and $HHgg$ vertices [33, 34] (see figure 2a) and C_2 the universal top-Yukawa-induced correction related to the Higgs wave-function and vacuum expectation value [35–38] (see figure 2b).[1] This yields the explicit effective Hgg and $HHgg$ couplings,

$$
\mathcal{L}_{\rm eff} = \frac{\alpha_s}{12\pi} G^{a\mu\nu} G^a_{\mu\nu} \left\{ (1+\delta_1)\frac{H}{v} + (1+\eta_1)\frac{H^2}{2v^2} + \mathcal{O}(H^3) \right\} \tag{3.3}
$$

where

$$
\delta_1 = \frac{x_t}{2} + \mathcal{O}(x_t^2)\,, \qquad\qquad \eta_1 = 4x_t + \mathcal{O}(x_t^2)\,. \tag{3.4}
$$

This effective Lagrangian describes the electroweak corrections induced by x_t to the Hgg and $HHgg$ vertices in the HTL and will be used in this limit in the following. We would like to point out explicitly that the square root of the wave-function counterterm of the external Higgs boson(s) is already taken into account in this effective Lagrangian.

3.2 Higgs self-couplings

The starting point of effective Higgs self-couplings is the effective one-loop corrected Higgs potential involving virtual top-quark effects of the SM [39–41],

$$
\begin{aligned}
V_{\rm eff} &= V_0 + V_1 \\
V_0 &= \mu_0^2 |\phi|^2 + \frac{\lambda_0}{2}|\phi|^4 \\
V_1 &= \frac{3\overline{m}_t^4}{16\pi^2} C_\epsilon \left(\frac{1}{\epsilon} + \log\frac{\bar{\mu}^2}{\overline{m}_t^2} + \frac{3}{2} \right)\,,
\end{aligned} \tag{3.5}
$$

with the bare Higgs self-coupling λ_0, the SM Higgs doublet in unitary gauge,

$$
\phi = \frac{1}{\sqrt{2}} \begin{pmatrix} 0 \\ v+H \end{pmatrix} \tag{3.6}
$$

the loop coefficient

$$
C_\epsilon = \Gamma(1+\epsilon)(4\pi^2)^\epsilon \tag{3.7}
$$

and the field-dependent top-mass parameter

$$
\overline{m}_t = m_t \left(1 + \frac{H}{v} \right)\,. \tag{3.8}
$$

[1]The coefficient C_1 corresponds to the genuine vertex corrections $\delta_1 + \delta_2$ of ref. [33] and C_2 to the universal corrections of ref. [35] that are denoted as δ_3 in ref. [33].

JHEP10(2022)185

The expression above for the effective Higgs potential involves the 't Hooft scale $\bar{\mu}$. After minimization of the effective Higgs potential by the tadpole equation,

$$\begin{aligned}\mu_0^2 &= -\frac{\lambda_0}{2}v^2 + \delta\mu^2 \\ \delta\mu^2 &= -\frac{3m_t^4}{4\pi^2 v^2}C_\epsilon\left\{\frac{1}{\epsilon} + \log\frac{\bar{\mu}^2}{m_t^2} + 1\right\}\end{aligned} \tag{3.9}$$

and the renormalization of the Higgs mass,

$$\begin{aligned}M_{H0}^2 &= \lambda_0 v^2 = \lambda v^2 + (\delta\lambda)v^2 = \lambda v^2 + \delta M_H^2 \\ \delta M_H^2 &= -\frac{3m_t^4}{2\pi^2 v^2}C_\epsilon\left\{\frac{1}{\epsilon} + \log\frac{\bar{\mu}^2}{m_t^2}\right\},\end{aligned} \tag{3.10}$$

the effective Higgs trilinear (quartic) self-coupling can be obtained by the third (fourth) derivative of this effective Higgs potential with respect to the physical Higgs field H,

$$\lambda_{HHH}^{\text{eff}} = 3\frac{M_H^2}{v} + \Delta\lambda_{HHH}\,, \qquad \lambda_{HHHH}^{\text{eff}} = 3\frac{M_H^2}{v^2} + \Delta\lambda_{HHHH}\,, \tag{3.11}$$

with

$$\Delta\lambda_{HHH} = -\frac{3m_t^4}{\pi^2 v^3}\,, \qquad \Delta\lambda_{HHHH} = -\frac{12m_t^4}{\pi^2 v^4}\,. \tag{3.12}$$

These effective NLO couplings are the relevant Higgs self-interactions in the HTL and will be compared with the full triple-vertex corrections within this work.

4 Top-Yukawa-induced electroweak corrections to Higgs pair production

The top-Yukawa-induced electroweak corrections arise from NLO diagrams involving top-quark loops as shown in figure 3, where the tadpole diagrams are displayed explicitly. For simplicity, we will use the relative corrections of eq. (3.3) to the ggH and $ggHH$ vertices in the HTL, while the radiative corrections to the triple-Higgs vertex and Higgs self-energies are treated with full top-mass dependence. Since there are no real corrections at the NLO electroweak level, the radiative corrections can be implemented by a shift of the LO form factors of eq. (2.3),

$$\begin{aligned}C_\triangle F_\triangle &\to C_\triangle F_\triangle(1+\Delta_\triangle) \\ F_\Box &\to F_\Box(1+\Delta_\Box)\,,\end{aligned} \tag{4.1}$$

while the LO form factor $G_\Box$ does not receive top-Yukawa-induced electroweak corrections in our approach, since $G_\Box$ vanishes in the HTL. The top-Yukawa-induced radiative corrections in eq. (4.1) read as[2]

$$\begin{aligned}\Delta_\triangle &= \delta_1 + \Delta_{HHH} \\ \Delta_\Box &= \eta_1\,,\end{aligned} \tag{4.2}$$

[2] It should be noted that in these expressions only δ_1 and η_1 are approximated in the HTL, while all other contributions include the full top-mass dependence, i.e. also the LO form factors $F_\triangle, F_\Box$ and $G_\Box$.

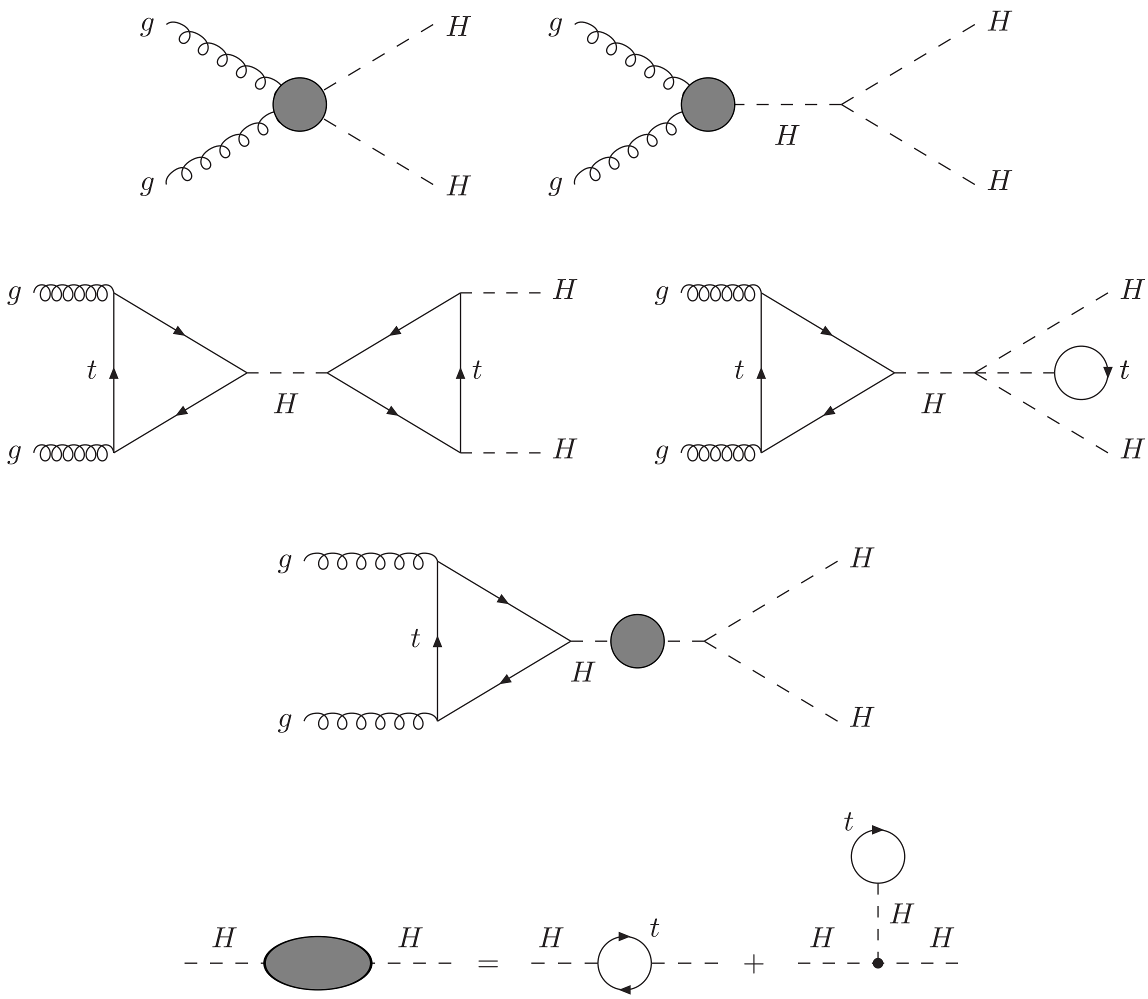

Figure 3. Generic diagrams describing the top-Yukawa-induced electroweak corrections to Higgs-boson pair production via gluon fusion. The blobs of the first two diagrams are determined by the effective Lagrangian of eq. (3.3) in the HTL.

where the vertex, self-energy and counterterm corrections are given by

$$
\begin{aligned}
\Delta_{HHH} &= \Delta_{\mathrm{vertex}} + \Delta_{\mathrm{self}} + \Delta_{\mathrm{CT}} \\
\Delta_{\mathrm{vertex}} &= \frac{m_t^4}{v^2 M_H^2} \frac{8}{(4\pi)^2} \Bigg\{ B_0(Q^2; m_t, m_t) + 2B_0(M_H^2; m_t, m_t) \\
&\qquad + \left(4m_t^2 - \frac{Q^2 + 2M_H^2}{2}\right) C_0(Q^2, M_H^2, M_H^2; m_t, m_t, m_t) \Bigg\} + \frac{T_1}{v M_H^2} \\
\Delta_{\mathrm{self}} &= \frac{\Sigma_H(Q^2)}{Q^2 - M_H^2} + \frac{1}{2}\Sigma'_H(M_H^2) \\
\Delta_{\mathrm{CT}} &= \frac{\delta M_H^2}{Q^2 - M_H^2} + \frac{\delta \lambda_{HHH}}{\lambda_{HHH}} \,. \qquad (4.3)
\end{aligned}
$$

We are adopting the scalar integrals in $n = 4 - 2\epsilon$ dimensions,

$$\begin{aligned}
A_0(m) &= \frac{(4\pi)^2}{i}\,\bar{\mu}^{4-n}\int\frac{d^nk}{(2\pi)^n}\frac{1}{k^2-m^2}\\
B_0(p^2;m_1,m_2) &= \frac{(4\pi)^2}{i}\,\bar{\mu}^{4-n}\int\frac{d^nk}{(2\pi)^n}\frac{1}{(k^2-m_1^2)[(k+p)^2-m_2^2]}\\
B_0'(p^2;m_1,m_2) &= \frac{\partial}{\partial p^2}B_0(p^2;m_1,m_2)\\
C_0(p_1^2,p_2^2,(p_1+p_2)^2;m_1,m_2,m_3) &= \frac{(4\pi)^2}{i}\,\bar{\mu}^{4-n}\int\frac{d^nk}{(2\pi)^n}\frac{1}{(k^2-m_1^2)[(k+p_1)^2-m_2^2]}\\
&\quad\times\frac{1}{[(k+p_1+p_2)^2-m_3^2]}\,. \qquad (4.4)
\end{aligned}$$

In the expression of eq. (4.3), the self-energy $\Sigma_H(Q^2)$ and its derivative $\Sigma_H'(Q^2)$, the tadpole term T_1/v, the trilinear Higgs-coupling counterterm $\delta\lambda_{HHH}$ and the Higgs-mass counterterm δM_H^2 are given by

$$\begin{aligned}
\Sigma_H(Q^2) &= 3\,\frac{T_1}{v} + 6\,\frac{m_t^2}{(4\pi)^2v^2}\Big\{2A_0(m_t) + (4m_t^2-Q^2)B_0(Q^2;m_t,m_t)\Big\} + \mathcal{O}(m_t^0)\\
\Sigma_H'(Q^2) &= 6\,\frac{m_t^2}{(4\pi)^2v^2}\Big\{(4m_t^2-Q^2)B_0'(Q^2;m_t,m_t) - B_0(Q^2;m_t,m_t)\Big\} + \mathcal{O}(m_t^0)\\
\frac{T_1}{v} &= -12\,\frac{m_t^2}{(4\pi)^2v^2}A_0(m_t)\\
\frac{\delta\lambda_{HHH}}{\lambda_{HHH}} &= \frac{\delta M_H^2}{M_H^2} + \frac{1}{2}\frac{\Sigma_W(0)}{M_W^2}\\
\frac{\Sigma_W(0)}{M_W^2} &= 2\,\frac{T_1}{vM_H^2} + \frac{2m_t^2}{(4\pi)^2v^2}\Big\{B_0(0;m_t,0) + 2B_0(0;m_t,m_t) + m_t^2B_0'(0;m_t,0)\Big\} + \mathcal{O}(m_t^0)\\
\delta M_H^2 &= -\Sigma_H(M_H^2)\,, \qquad (4.5)
\end{aligned}$$

where the self-energies Σ_H, Σ_W and the Higgs-mass counterterm include tadpole contributions as well, and we only kept terms of $\mathcal{O}(m_t^4)$ and $\mathcal{O}(m_t^2)$ for the counterterms to be consistent. For the calculation, we have used the alternative tadpole-scheme of ref. [42][3] and implemented the electroweak parameters in the G_F scheme, i.e. choosing G_F, M_Z, M_W as input parameters for the electroweak gauge sector, while the Weinberg angle θ_W and the QED coupling α are derived quantities. In addition, we have taken into account that the effective Lagrangian of eq. (3.3) contains the wave-function renormalization of the external Higgs fields that has to be compensated in the corrections Δ_{HHH} to avoid double counting. Within our electroweak renormalization, the trilinear coupling is given by its LO expression in terms of the renormalized Higgs mass and vacuum expectation value of eq. (2.5). We will compare the explicit NLO result of eq. (4.1) to the corresponding one

[3] We have checked explicitly that in the conventional approach of using a tadpole counterterm to cancel all tadpole diagrams, we arrive at the same result for Δ_{HHH} due to the residual tadpole contribution to the counterterm for the trilinear Higgs coupling λ_{HHH} [43].

JHEP10(2022)185

using the effective trilinear coupling $\lambda^{\rm eff}_{HHH}$, i.e. adding the corresponding matching term

$$\begin{aligned}\Delta_{HHH} &\to \Delta_{HHH} + \Delta_\lambda \\ \Delta_\lambda &= -\frac{\Delta\lambda_{HHH}}{\lambda_{HHH}} = 16\frac{m_t^4}{(4\pi)^2 v^2 M_H^2}\end{aligned} \tag{4.6}$$

with $\Delta\lambda_{HHH}$ of eq. (3.12) to avoid double counting and using the effective coupling $\lambda_{HHH} \to \lambda^{\rm eff}_{HHH}$ of eq. (3.11) for the triangle coefficient $C_\triangle$ in eq. (2.3) in both the LO and NLO expressions.

The relative electroweak corrections to the Higgs-pair production cross section are defined by expanding the expression of eq. (2.3) up to NLO by using the corrected form factors of eq. (4.1) at the parton level,

$$\begin{aligned}\hat\sigma_{NLO} &= \hat\sigma_{LO} + \Delta\hat\sigma \\ \Delta\hat\sigma &= \frac{G_F^2\alpha_s^2(\mu_R)}{512(2\pi)^3}\int_{\hat t_-}^{\hat t_+} d\hat t\; 2\Re e\left\{(C_\triangle F_\triangle + F_\Box)^*(C_\triangle F_\triangle \Delta_\triangle + F_\Box \Delta_\Box)\right\}\end{aligned} \tag{4.7}$$

such that the hadronic cross section is corrected as

$$\begin{aligned}\sigma_{NLO} &= \sigma_{LO}\,(1+\delta_{\rm elw}) \\ \delta_{\rm elw} &= \frac{\Delta\sigma}{\sigma_{LO}} \\ \Delta\sigma &= \int_{\tau_0}^1 \frac{\mathcal{L}^{gg}}{d\tau}\Delta\hat\sigma\end{aligned} \tag{4.8}$$

Within this expression we will either use the LO expression of the triple Higgs coupling λ_{HHH} of eq. (2.5) or the radiatively-corrected effective coupling $\lambda^{\rm eff}_{HHH}$ of eq. (3.11) with the according form of the radiative corrections as shown in eq. (4.6).

5 Results

For our numerical analysis we work at a c.m. energy of 14 TeV at the LHC and use a top pole mass of $m_t = 172.5$ GeV according to the conventions of the LHC Higgs Working Group [44]. The Fermi constant is chosen as $G_F = 1.1663787 \times 10^{-5}$ GeV^{-2}, the strong coupling as $\alpha_s(M_Z) = 0.118$ and the Higgs mass as $M_H = 125$ GeV. We are using PDF4LHC15 parton densities.

The (complex) electroweak correction factor Δ_{HHH} of eq. (4.3) is shown in figure 4 as a function of the invariant Higgs-pair mass M_{HH}. The full lines denote the real parts and the dashed line the imaginary part. The blue curves exhibit the real and imaginary parts of Δ_{HHH} in terms of the LO trilinear Higgs coupling, while the red curve shows the correction factor after introducing the effective coupling $\lambda^{\rm eff}_{HHH}$. The size of the correction factor shows that the effective trilinear coupling does not capture the dominant part of the electroweak corrections so that its use is not supported by our results.

The relative electroweak corrections originating from the top-Yukawa-induced contributions are shown in figure 5 for the differential cross section as a function of the invariant Higgs-pair mass M_{HH}. The radiative corrections close to the production threshold turn

JHEP10(2022)185

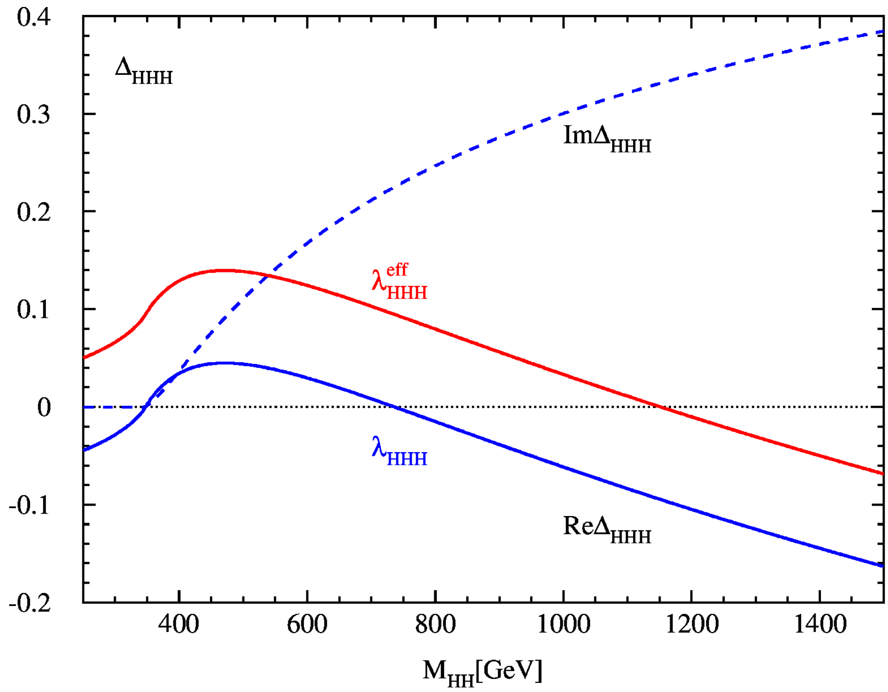

Figure 4. The relative top-Yukawa-induced electroweak correction factor Δ_{HHH} as a function of the invariant Higgs-pair mass M_{HH}. The full blue curve shows the real part of Δ_{HHH} and the dashed blue on the imaginary part. The red curve exhibits the real part after introducing the effective trilinear coupling $\lambda^{\rm eff}_{HHH}$ of eq. (3.11) and adding the shift of eq. (4.6). To guide the eye the dotted black curve has been added as the zero-line.

out to be large. To understand this behaviour, it is important to recall that the LO form factors of the matrix element vanish in the HTL due to the complete cancellation of the triangle and box form factors $F_\triangle, F_\Box$, i.e. the leading term of a heavy-top expansion is equal to zero. Thus, the form factors arise from the subleading $\mathcal{O}(1/m_t^2)$ terms and are thus suppressed close to threshold at LO. Therefore the top-Yukawa induced electroweak corrections are large near the production threshold, since they lift the cancellation of the leading term of the heavy-top expansion due to introducing an imbalance between the triangle and box diagrams.

This suppression, however, is lifted by the radiative corrections to the effective trilinear Higgs coupling $\lambda^{\rm eff}_{HHH}$ or, equivalently, the mismatch of electroweak corrections to the triangle and box diagrams. However, figure 5 does not support the use of the effective trilinear Higgs coupling $\lambda^{\rm eff}_{HHH}$ to improve the perturbative result. Thus, the naive argument that the effective trilinear Higgs coupling induces a SM contribution to κ_λ,

$$\begin{aligned} \lambda^{\rm eff}_{HHH} &= \kappa_\lambda \lambda_{HHH} \\ \lambda_{HHH} &= 3\,\frac{M_H^2}{v} \\ \kappa_\lambda &= 1 - \frac{m_t^4}{\pi^2 v^2 M_H^2} \approx 0.91 \end{aligned} \tag{5.1}$$

JHEP10(2022)185

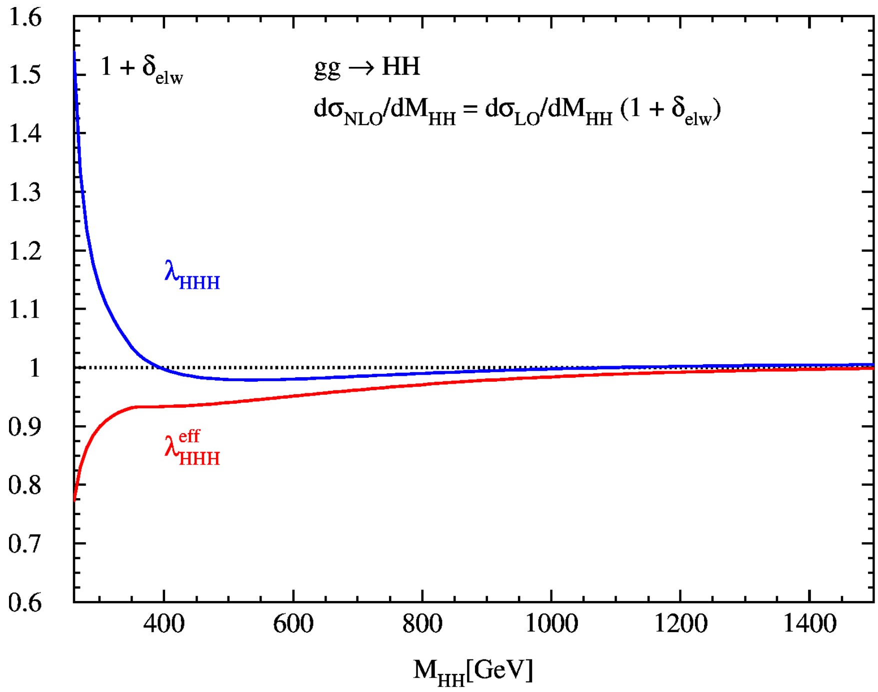

Figure 5. The relative top-Yukawa-induced electroweak corrections to the differential Higgs-pair production cross section as a function of the invariant Higgs-pair mass M_{HH}. The blue curve shows the electroweak correction factor using the LO trilinear Higgs coupling of eq. (2.5) and the red curve the corrections factor involving the effective coupling $\lambda^{\text{eff}}_{HHH}$ of eq. (3.11). The black dotted line at the value 1 is inserted to guide the eye. The electroweak corrections factor is independent of the hadronic c.m. energy and scale choices in the QCD part of the differential cross section $d\sigma/dM_{HH}$ so that it is valid for any hadronic energy as a pure rescaling factor.

is not supported by our results, but the inclusion of the complete electroweak corrections is mandatory instead. We observe that the electroweak corrections appear with opposite sign close to the threshold between the options of using the LO and the effective trilinear coupling.

The effect of the top-Yukawa-induced electroweak corrections on the total integrated hadronic cross section amounts to

$$\begin{aligned} \sigma &= K_{\text{elw}} \times \sigma_{LO} \\ K_{\text{elw}} &\approx 1.002 && (\lambda_{HHH}) \\ K^{\text{eff}}_{\text{elw}} &\approx 0.938 && (\lambda^{\text{eff}}_{HHH}) \end{aligned} \tag{5.2}$$

so that the corrections induce an effect of about 0.2% on the total cross section, if the LO-like trilinear Higgs coupling λ_{HHH} is adopted. The bulk of these corrections *cannot* be absorbed in the effective triple Higgs coupling, but the latter option leads to an artificial increase of the relative electroweak corrections. The reason behind these findings is that the external momentum-dependent corrections are of the same size as the corrections from the effective Higgs potential so that the latter are not dominant.

6 Conclusions

In this note we have investigated the electroweak corrections to Higgs-pair production via gluon fusion induced by top-quark contributions. While keeping the full top-mass dependence in the triple-Higgs vertex and self-energy corrections, we have worked in the HTL for the radiative corrections to the effective $ggH(H)$ vertices for the relative corrections. The top-Yukawa-induced NLO electroweak corrections to the total gluon-fusion cross section amount to about 0.2%. After integrating out the top-quark contributions an effective trilinear Higgs coupling can be defined in terms of the effective Higgs potential that is dressed with contributions scaling with the fourth power of the top mass. This is known already starting from the Coleman-Weinberg potential [39–41]. This effective trilinear Higgs coupling can be introduced in the full calculation of electroweak corrections as well and leads to a modification of the counterterms in order to remove potential double counting of corrections. However, introducing this effective coupling the remaining electroweak corrections turn out to be larger than in the case of the LO-like triple Higgs coupling.

Acknowledgments

The authors are indebted to A. Djouadi and P. Gambino for very helpful discussions. The research of M.M. is supported by the Deutsche Forschungsgemeinschaft (DFG, German Research Foundation) under grant 396021762-TRR 257. The work of J.S. is supported by the Swiss National Science Foundation (SNSF).

JHEP10(2022)185

References

[1] ATLAS collaboration, *Observation of a new particle in the search for the Standard Model Higgs boson with the ATLAS detector at the LHC*, Phys. Lett. B **716** (2012) 1 [arXiv:1207.7214] [INSPIRE].

[2] CMS collaboration, *Observation of a new boson at a mass of* 125 *GeV with the CMS experiment at the LHC*, Phys. Lett. B **716** (2012) 30 [arXiv:1207.7235] [INSPIRE].

[3] ATLAS and CMS collaborations, *Measurements of the Higgs boson production and decay rates and constraints on its couplings from a combined ATLAS and CMS analysis of the LHC pp collision data at* $\sqrt{s} = 7$ *and* 8 *TeV*, JHEP **08** (2016) 045 [arXiv:1606.02266] [INSPIRE].

[4] ATLAS collaboration, *Combined measurements of Higgs boson production and decay using up to* 80 fb^{-1} *of proton-proton collision data at* $\sqrt{s} = 13$ *TeV collected with the ATLAS experiment*, Tech. Rep. ATLAS-CONF-2019-005, CERN, Geneva, Switzerland (2019).

[5] CMS collaboration, *Evidence for Higgs boson decay to a pair of muons*, JHEP **01** (2021) 148 [arXiv:2009.04363] [INSPIRE].

[6] ALEPH, DELPHI, L3, OPAL and LEP Electroweak Working Group collaborations, *Precision electroweak measurements and constraints on the Standard Model*, arXiv:0712.0929 [INSPIRE].

[7] G. 't Hooft, *Renormalizable Lagrangians for massive Yang-Mills fields*, Nucl. Phys. B **35** (1971) 167 [INSPIRE].

[8] G. 't Hooft and M.J.G. Veltman, *Regularization and renormalization of gauge fields*, Nucl. Phys. B **44** (1972) 189 [INSPIRE].

[9] C.H. Llewellyn Smith, *High-energy behavior and gauge symmetry*, Phys. Lett. B **46** (1973) 233 [INSPIRE].

[10] J.M. Cornwall, D.N. Levin and G. Tiktopoulos, *Derivation of gauge invariance from high-energy unitarity bounds on the s matrix*, Phys. Rev. D **10** (1974) 1145 [*Erratum ibid.* **11** (1975) 972] [INSPIRE].

[11] B.W. Lee, C. Quigg and H.B. Thacker, *The strength of weak interactions at very high-energies and the Higgs boson mass*, Phys. Rev. Lett. **38** (1977) 883 [INSPIRE].

[12] B.W. Lee, C. Quigg and H.B. Thacker, *Weak interactions at very high-energies: the role of the Higgs boson mass*, Phys. Rev. D **16** (1977) 1519 [INSPIRE].

[13] J. Baglio, A. Djouadi, R. Gröber, M.M. Mühlleitner, J. Quevillon and M. Spira, *The measurement of the Higgs self-coupling at the LHC: theoretical status*, JHEP **04** (2013) 151 [arXiv:1212.5581] [INSPIRE].

[14] J. Alison et al., *Higgs boson potential at colliders: status and perspectives*, Rev. Phys. **5** (2020) 100045 [arXiv:1910.00012] [INSPIRE].

[15] S. Dawson, S. Dittmaier and M. Spira, *Neutral Higgs boson pair production at hadron colliders: QCD corrections*, Phys. Rev. D **58** (1998) 115012 [hep-ph/9805244] [INSPIRE].

[16] A. Djouadi, W. Kilian, M. Mühlleitner and P.M. Zerwas, *Production of neutral Higgs boson pairs at LHC*, Eur. Phys. J. C **10** (1999) 45 [hep-ph/9904287] [INSPIRE].

[17] S. Borowka et al., *Higgs boson pair production in gluon fusion at next-to-leading order with full top-quark mass dependence*, Phys. Rev. Lett. **117** (2016) 012001 [*Erratum ibid.* **117** (2016) 079901] [arXiv:1604.06447] [INSPIRE].

[18] S. Borowka et al., *Full top quark mass dependence in Higgs boson pair production at NLO*, JHEP **10** (2016) 107 [arXiv:1608.04798] [INSPIRE].

[19] J. Baglio, F. Campanario, S. Glaus, M. Mühlleitner, M. Spira and J. Streicher, *Gluon fusion into Higgs pairs at NLO QCD and the top mass scheme*, Eur. Phys. J. C **79** (2019) 459 [arXiv:1811.05692] [INSPIRE].

[20] J. Baglio et al., *Higgs-pair production via gluon fusion at hadron colliders: NLO QCD corrections*, JHEP **04** (2020) 181 [arXiv:2003.03227] [INSPIRE].

[21] J. Baglio, F. Campanario, S. Glaus, M. Mühlleitner, J. Ronca and M. Spira, *$gg \to HH$: combined uncertainties*, Phys. Rev. D **103** (2021) 056002 [arXiv:2008.11626] [INSPIRE].

[22] D. de Florian and J. Mazzitelli, *Two-loop virtual corrections to Higgs pair production*, Phys. Lett. B **724** (2013) 306 [arXiv:1305.5206] [INSPIRE].

[23] D. de Florian and J. Mazzitelli, *Higgs boson pair production at next-to-next-to-leading order in QCD*, Phys. Rev. Lett. **111** (2013) 201801 [arXiv:1309.6594] [INSPIRE].

[24] J. Grigo, K. Melnikov and M. Steinhauser, *Virtual corrections to Higgs boson pair production in the large top quark mass limit*, Nucl. Phys. B **888** (2014) 17 [arXiv:1408.2422] [INSPIRE].

JHEP10(2022)185

[25] M. Grazzini et al., *Higgs boson pair production at NNLO with top quark mass effects*, *JHEP* **05** (2018) 059 [arXiv:1803.02463] [INSPIRE].

[26] L.-B. Chen, H.T. Li, H.-S. Shao and J. Wang, *Higgs boson pair production via gluon fusion at N^3LO in QCD*, *Phys. Lett. B* **803** (2020) 135292 [arXiv:1909.06808] [INSPIRE].

[27] L.-B. Chen, H.T. Li, H.-S. Shao and J. Wang, *The gluon-fusion production of Higgs boson pair: N^3LO QCD corrections and top-quark mass effects*, *JHEP* **03** (2020) 072 [arXiv:1912.13001] [INSPIRE].

[28] J. Grigo, J. Hoff and M. Steinhauser, *Higgs boson pair production: top quark mass effects at NLO and NNLO*, *Nucl. Phys. B* **900** (2015) 412 [arXiv:1508.00909] [INSPIRE].

[29] D.Y. Shao, C.S. Li, H.T. Li and J. Wang, *Threshold resummation effects in Higgs boson pair production at the LHC*, *JHEP* **07** (2013) 169 [arXiv:1301.1245] [INSPIRE].

[30] D. de Florian and J. Mazzitelli, *Higgs pair production at next-to-next-to-leading logarithmic accuracy at the LHC*, *JHEP* **09** (2015) 053 [arXiv:1505.07122] [INSPIRE].

[31] E.W.N. Glover and J.J. van der Bij, *Higgs boson pair production via gluon fusion*, *Nucl. Phys. B* **309** (1988) 282 [INSPIRE].

[32] T. Plehn, M. Spira and P.M. Zerwas, *Pair production of neutral Higgs particles in gluon-gluon collisions*, *Nucl. Phys. B* **479** (1996) 46 [*Erratum ibid.* **531** (1998) 655] [hep-ph/9603205] [INSPIRE].

[33] A. Djouadi and P. Gambino, *Leading electroweak correction to Higgs boson production at proton colliders*, *Phys. Rev. Lett.* **73** (1994) 2528 [hep-ph/9406432] [INSPIRE].

[34] K.G. Chetyrkin, B.A. Kniehl and M. Steinhauser, *Three loop $O(\alpha_S^2 G_F M_t^2)$ corrections to hadronic Higgs decays*, *Nucl. Phys. B* **490** (1997) 19 [hep-ph/9701277] [INSPIRE].

[35] B.A. Kniehl, *Radiative corrections for $H \to f\bar{f}(\gamma)$ in the standard model*, *Nucl. Phys. B* **376** (1992) 3 [INSPIRE].

[36] B.A. Kniehl and M. Spira, *Two loop $O(\alpha_s G_F m_t^2)$ correction to the $H \to b\bar{b}$ decay rate*, *Nucl. Phys. B* **432** (1994) 39 [hep-ph/9410319] [INSPIRE].

[37] B.A. Kniehl and M. Spira, *Low-energy theorems in Higgs physics*, *Z. Phys. C* **69** (1995) 77 [hep-ph/9505225] [INSPIRE].

[38] A. Kwiatkowski and M. Steinhauser, *Corrections of order $O(G_F \alpha_s m_t^2)$ to the Higgs decay rate $\Gamma(H \to b\bar{b})$*, *Phys. Lett. B* **338** (1994) 66 [*Erratum ibid.* **342** (1995) 455] [hep-ph/9405308] [INSPIRE].

[39] S.R. Coleman and E.J. Weinberg, *Radiative corrections as the origin of spontaneous symmetry breaking*, *Phys. Rev. D* **7** (1973) 1888 [INSPIRE].

[40] S. Weinberg, *Perturbative calculations of symmetry breaking*, *Phys. Rev. D* **7** (1973) 2887 [INSPIRE].

[41] R. Jackiw, *Functional evaluation of the effective potential*, *Phys. Rev. D* **9** (1974) 1686 [INSPIRE].

[42] J. Fleischer and F. Jegerlehner, *Radiative corrections to Higgs decays in the extended Weinberg-Salam model*, *Phys. Rev. D* **23** (1981) 2001 [INSPIRE].

[43] A. Denner and S. Dittmaier, *Electroweak radiative corrections for collider physics*, *Phys. Rept.* **864** (2020) 1 [arXiv:1912.06823] [INSPIRE].

[44] LHC Higgs Cross Section Working Group collaboration, *Handbook of LHC Higgs cross sections: 4. Deciphering the nature of the Higgs sector*, arXiv:1610.07922 [INSPIRE].

JHEP10(2022)185